

Synthesis of bicyclic molecular scaffolds (BTAA): An investigation towards new selective MMP-12 inhibitors

Claudia Mannino,^{a,d} Marco Nievo,^a Fabrizio Machetti,^c Athanasios Papakyriakou,^d
Vito Calderone,^d Marco Fragai^{d,e} and Antonio Guarna^{a,b,*}

^aDepartment of Organic Chemistry “U. Schiff”, University of Florence, 50019 Sesto Fiorentino (FI), Italy

^bLaboratory of Design, Synthesis and Study of Biologically Active Heterocycles (HeteroBioLab) Via della Lastruccia 13, 50019 Sesto Fiorentino (FI), Italy

^cIstituto di chimica dei composti organometallici del CNR c/o Dipartimento di Chimica Organica ‘U. Schiff’, Firenze, Italy

^dCenter of Magnetic Resonance (CERM), University of Florence, Via Sacconi 6, 50019 Sesto Fiorentino (FI), Italy

^eDepartment of Agricultural Biotechnology (DIBA), University of Florence, Via Maragliano 75, 50144 Florence, Italy

Received 6 March 2006; revised 3 July 2006; accepted 10 July 2006

Available online 8 August 2006

Abstract—Starting from 3-aza-6,8-dioxo-bicyclo[3.2.1]octane scaffold (BTAA) a virtual library of molecules was generated and screened in silico against the crystal structure of the Human Macrophage Metalloelastase (MMP-12). The molecules obtaining high score were synthesized and the affinity for the catalytic domain of MMP-12 was experimentally proved by NMR experiments. A BTAA scaffold **20** having a *N*-hydroxyurea group in position 3 and a *p*-phenylbenzylcarboxy amide in position 7 showed a fair inhibition potency ($IC_{50} = 149 \mu M$) for MMP-12 and some selectivity towards five different MMPs. These results, taken together with the X-ray structure of the adduct between MMP-12, the inhibitor **20** and the acetohydroxamic acid (AHA), suggest that bicyclic scaffold derivatives may be exploited for the design of new selective matrix metalloproteinase inhibitors (MMPIs).

© 2006 Elsevier Ltd. All rights reserved.

1. Introduction

Matrix metalloproteinases (MMPs) are a family of zinc-dependent, calcium containing, endopeptidases involved in extracellular matrix degradation and, consequently, they play a crucial role in physiological processes such as tissue remodelling and healing of wounds.¹ As the upregulation of MMPs is involved in many inflammatory, malignant and degenerative diseases,² attempts to design and develop inhibitors that may modulate their regulation have become of great interest.^{3–5}

The main requirement for a small molecule to be an effective metalloproteinase inhibitor (MMPI) is the presence of both a functional group capable of chelating the active-site zinc ion and a lipophilic residue able to fit into the S'_1 pocket.⁴ Hydroxamic acid is the most popular zinc binding group (ZBG) for MMPIs even if some authors report that it is fast metabolized in vivo^{6,7} and

it contributes to increase toxicity due to its low metal binding selectivity.⁸

The inhibitors designed up to date usually bind the active site on the catalytic domain providing nanomolar dissociation constants.^{3,4} However, several inhibitors exhibit a poor selectivity as a consequence of the high structural similarity among the members of the MMP family.⁹ Even if the low specificity does not prevent the use in vivo, it raises a lot of side effects and it also limits the dose that may be daily administered.^{10,11} As a consequence, the search of new potent and selective MMP inhibitors still represents an important pharmaceutical target.

Even if the expensive high-throughput screening of small molecule libraries is one of the most popular approaches in pharmaceutical research, alternative strategies, based on docking calculation and rational drug design, may be adopted if the 3D structure of the target is solved.^{12–14}

A new class of molecular heterocyclic scaffolds (BTAA) based on 3-aza-6,8-dioxo-bicyclo[3.2.1]octane skeleton,¹⁵ which can be decorated with a ZBG and a

Keywords: Metalloproteinases; Inhibitors; BTAA; NMR spectroscopy.

* Corresponding author. Tel.: +39 055 4573481; fax: +39 055 4573569; e-mail: antonio.guarna@unifi.it

lipophilic residue, was chosen to design selective MMP-12 inhibitors (Fig. 1).

The main feature of these scaffolds is their tridimensional bicyclic skeleton generated by combination of sugar and amino acid derivatives. Their synthesis includes only few steps starting from commercially available enantiopure precursors and a stereochemistry control can be accomplished in each step of the synthesis. As dipeptide isosteres, BTAs are compounds with potential biological activity and their use as central core of pharmaceutical targets is convenient as a high number of positions can be functionalized leading to molecular diversity. Limited flexibility can be advantageous to correctly direct the pharmacophore side chains and it is also useful for computational analysis. In addition, as amino acids, they have full compatibility with the conditions required for solid-phase synthesis.^{15,16}

All these properties, together with fair solubility and low molecular weight, were considered in scaffold selection.

Diversification of BTAs by easy decoration with different functional groups may generate virtual libraries which may be screened *in silico* in order to identify new hit compounds for further lead discovery. Even if the binding energy provided by docking programs does not reflect exactly the real binding affinity, its value al-

lows to score the docking results in order to identify a class of potential ligand.¹⁷

Moreover, the experimental assessment of the affinity of few selected molecules outlined by docking results gives the chance to correlate binding energies and binding constants improving the prediction reliability. A combined use of virtual screening and experimental determination of the binding affinity suggested that the BTAs may represent a new type of scaffolds to design a new class of MMPis.

2. Chemistry

The synthesis of 3-biphenyl-4-ylmethyl-3-aza-6,8-dioxabicyclo[3.2.1]octane-7-carboxylic acid methyl ester (*p*-PhBn-BTGOME) (**8**) was carried out following a procedure previously reported for similar compounds and is briefly reported below Scheme 1.¹²

Reductive alkylation of aminoacetal **1** with biphenyl-4-carbaldehyde (**2**) and NaBH₄ afforded in good yield the aryl aminoacetal **3** which was subsequently converted into the amide **5** by treatment with (*R,R*) tartaric anhydride¹⁸ **4**. Crude **5** was treated with thionyl chloride in MeOH affording cyclic acetal **6**, which was submitted to the acid-catalyzed cyclization to give **7** in 40% yield over the four steps. Reduction of amide **7** with BH₃·Me₂S furnished the corresponding amine **8** in 70% yield (Scheme 1).

Basic hydrolysis of **7** and acid-catalyzed hydrolysis of **8** gave, respectively, the free acids **9** and **10** in good yields.

A peculiar feature of BTAs is the demonstrated high reactivity of their methyl ester function towards amines, although simple esters are usually not very reactive towards direct aminolysis.¹⁹ Owing to this, hydroxamic acids **11** and **12** were easily prepared by mixing the scaffold

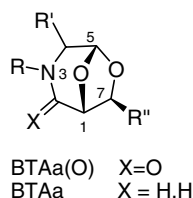
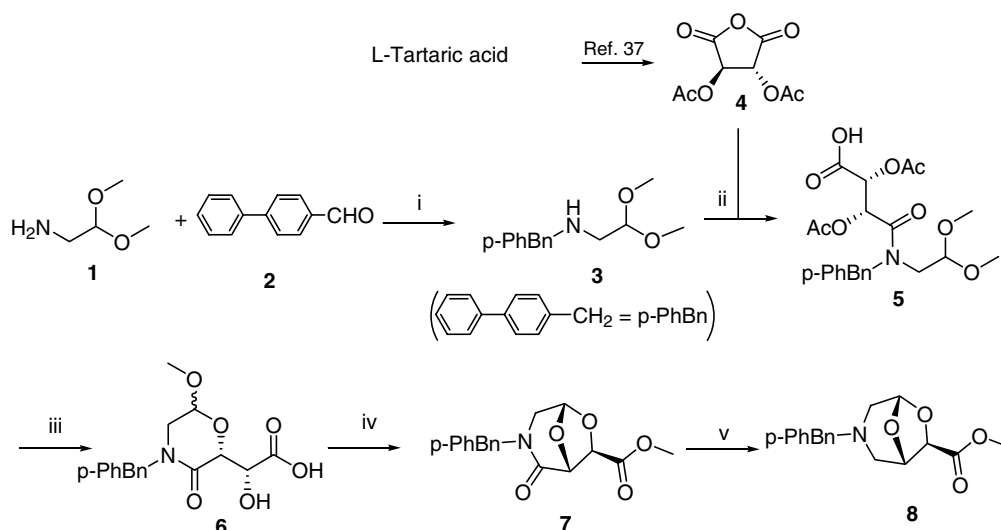
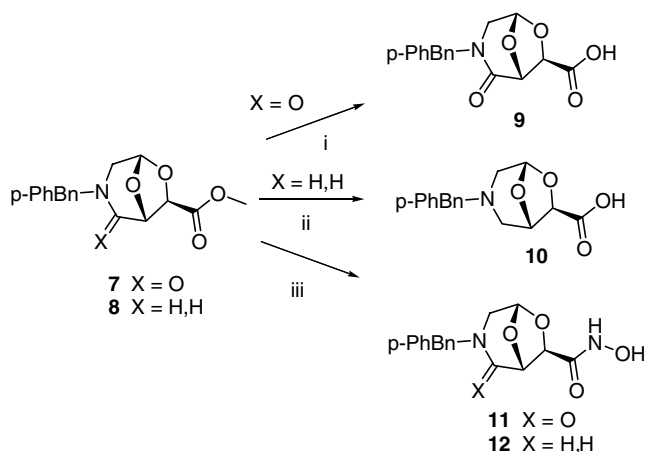


Figure 1.



Scheme 1. Reagents and conditions: (i) NaBH₄, MeOH, 25 °C, 16 h; (ii) CH₂Cl₂, 25 °C, 16 h; (iii) SOCl₂, MeOH, 60 °C, 2 h; (iv) H₂SO₄/SiO₂, toluene, reflux, 20 min, 41% (over the four steps); (v) BH₃·Me₂S, THF, 25 °C, 16 h, 70%.



Scheme 2. Reagents and conditions: (i) LiOH, MeOH/THF, 25 °C, 12 h, 80%; (ii) HCl 4 M, 25 °C, 12 h, 90%; (iii) $\text{NH}_2\text{OH}\cdot\text{HCl}$, NEt_3 , CHCl_3 , 25 °C, 48 h, 21% (**11**), 26% (**12**).

with an excess of hydroxylamine hydrochloride (5 equiv) and NEt_3 in CHCl_3 at room temperature (Scheme 2).

To prepare the model compound **15** having a *N*-hydroxyurea as zinc-binding group, piperidine **13** was treated with triphosgene and then with benzyl-hydroxylamine and NEt_3 affording compound **14**. The debenzylated product **15** was readily obtained by mild hydrogenolytic cleavage of the protecting group over 5% Pd/C at 1 atm (Scheme 3).²⁰

A new BTAA scaffold **20** having the *N*-hydroxyurea group in position 3 and the *p*-phenylbenzylcarboxy amide in position 7 was then prepared. Due to the high reactivity of ester **16**, the biphenyl derivative **17** was easily and quantitatively prepared by stirring the starting material at 60 °C with a neat excess of amine. Debonylation was carried out by refluxing a solution of **17** in MeOH in the presence of ammonium formate and catalytic Pd/C. Then, compound **18** was activated with carbonyldiim-

idazole (CDI) and treated with *O*-benzylhydroxylamine, as a free base, providing the substituted *N*-hydroxyurea **19** in 60% yield after crystallization.²¹ Hydrogenolytic cleavage of the benzyl group over 5% Pd/C afforded the desired final compound **20** (Scheme 4).

3. Results and discussion

The availability of high-resolution structure of the MMP-12 catalytic domain^{22,23} provided the possibility to employ a structure-based approach to design and screen a virtual library.

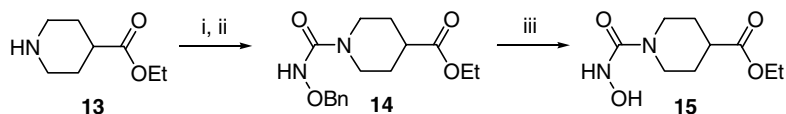
A biphenylic moiety and a hydroxamic (or carboxylic) acid were chosen as good substituents²⁴ to be introduced in different position of BTAA and hundreds of structures were so generated and tested in silico for their affinity to the catalytic domain of MMP-12.

The hits with the highest score were selected and, among them, compounds **9–12** were synthesized due to their higher feasibility. In this class of molecules the scaffold supports the biphenylic moiety in front of the ZBG. The Autodock binding model predicted a deep insertion of the biphenyl group into the S'_1 cavity though the coordination geometry of the ZBG appeared not to be optimized.

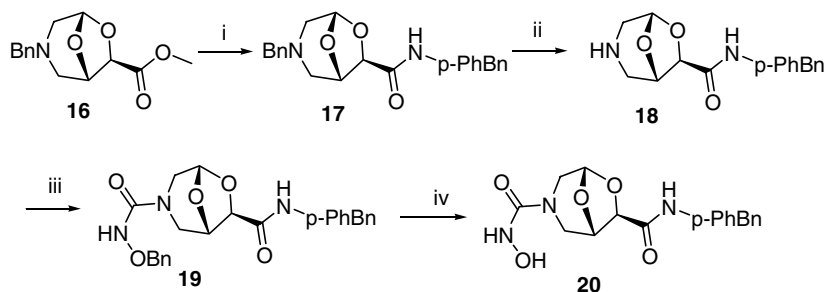
Dissociation constants (K_D) of compounds **9–12** were calculated through ^{15}N – ^1H HSQC experiments.²⁵ In addition, compounds **21–24**, already present in our chemical library, were submitted to the same experiments in order to compare the results and support the docking model.

Moreover, the inhibitory activity (IC_{50}) of compounds **9–12** was measured by enzymatic assays.²⁶

The values of K_D and IC_{50} for the tested compounds **9–12** and **20–24** are reported in Table 1.



Scheme 3. Reagents and conditions: (i) $(\text{CCl}_3\text{O})_2\text{CO}$, CH_2Cl_2 , from 0 °C to 25 °C, 12 h; (ii) $\text{Bn-O-NH}_2\cdot\text{HCl}$, NEt_3 , CH_2Cl_2 , 25 °C, 12 h, 40%; (iii) H_2 (1 atm), 5% Pd/C, AcOEt, 25 °C, 12 h, quantitative.



Scheme 4. Reagents and conditions: (i) *p*-PhBn– NH_2 , 60 °C, 12 h, 93%; (ii) HCO_2NH_4 , 10% Pd/C, MeOH, reflux, 2 h, 64%; (iii) BnONH_2 , CDI, THF, 25 °C, 12 h, 60%; (iv) H_2 (1 atm), 5% Pd/C, THF, 25 °C, 12 h, 68%.

Table 1. Calculated MMP-12 binding affinity (K_D) and inhibition potency (IC_{50})

Compound	X	R	R'	R''	MMP-12 K_D^c	MMP-12 IC_{50}^d (μ M)
9	O	<i>p</i> -PhBn	H	COOH	≥ 1 mM	954
10	H, H	<i>p</i> -PhBn	H	COOH	≥ 1 mM	835
11	O	<i>p</i> -PhBn	H	CONHOH	≥ 500 μ M	425
12	H, H	<i>p</i> -PhBn	H	CONHOH	≥ 500 μ M	399
20	H, H	HONHCO	H	CONH- <i>p</i> -PhBn	154 μ M	149
21^a	O	Bn	H	COOH	≥ 10 mM	—
22^a	H, H	Bn	H	COOH	≥ 10 mM	—
23^a	O	Bn	H	CONHOH	≥ 10 mM	—
24^a	H, H	<i>p</i> -PhBn	COOH	H	not detec. ^b	—

15

^a Compounds previously described.^{15,29,30}

^b No detectable interaction found by NMR.

^c Dissociation constants measured through ^{15}N - ^1H HSQC NMR experiments.

^d Inhibition potency measured by fluorescence enzymatic assays.

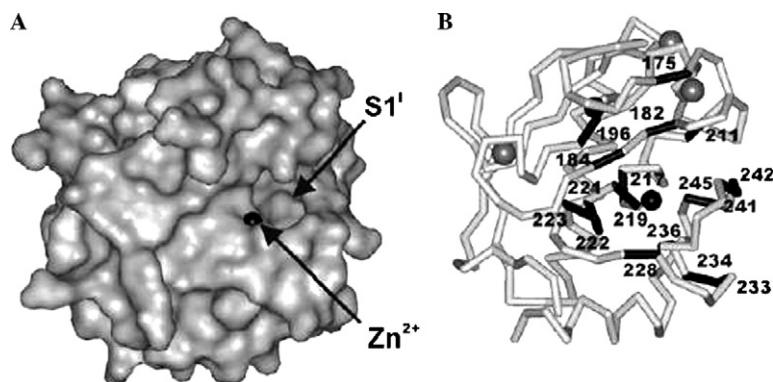


Figure 2. (A) Surface model of the MMP-12 showing the catalytic zinc and the S_1' pocket. (B) Residues of the MMP-12 affected by chemical shift perturbation upon the addition of **12**.

Since the identification of the amino acids involved in the binding may be crucial to prove a direct interaction with the catalytic site and, consequently, for the optimization of the process, NMR-based strategies were also used to localize the binding site on the target.²⁷ The identification of the binding site was easily performed analyzing the protein resonance chemical shifts in ^1H - ^{15}N HSQC spectra, recorded either in presence or in absence of the ligand.²⁸

The pattern of the shifts was similar for all ligands. Several residues forming the S_1' cavity, one or more zinc binding histidines and the neighbouring amino acids are strongly influenced by the presence of this class of molecules. As example, a ribbon representation of MMP-12 is shown in Figure 2. The NHs showing significant chemical shift perturbation upon the addition of compound **12** are highlighted. The affected amino acids nicely define the ligand binding site that is the same for all the designed compounds in agreement with the docking results. Only few differences were found among the

members of this class. In particular, the NH cross-peak of His218 was only weakly shifted by lactams **9** and **11** with respect to compound **12**.

The analysis of the results summarized in Table 1 suggests that the bicyclic skeleton of BTAA should be compatible with the metalloelastase catalytic domain, but the activity is strongly modulated by the type and position of the substituents. Hydroxamic acids **11**, **12** ($IC_{50} = 425$ μ M, 399 μ M, respectively) are more potent than the carboxylic ones **9**, **10** ($IC_{50} = 954$ μ M, 835 μ M, respectively). The affinity observed within this series seemed to be highly dependent on the presence of the biphenylic moiety: the replacement of the biphenylmethyl with a benzylic-protecting group resulted in a loss of binding affinity, so compounds **21** and **22** ($K_D \geq 10$ mM) are almost inactive; and the introduction of the hydroxamic moiety in position 7 did not restore the activity (see compound **23**). Otherwise, the presence of the ZBG and the lipophilic residue in vicinal position decreases the binding affinity as demonstrated

by compound **24** for which no detectable interactions were found by NMR.

With these results in our hands we decided to focus our efforts on the design of new derivatives with improved affinity. A deeper penetration in the S'_1 cavity was possible moving the biphenyl group quite far from the scaffold. Due to the high reactivity of the BTAA methyl ester, it was synthetically very easy to introduce the biphenylic moiety in **7** through an amide bond. As a consequence, the best anchoring point for the ZBG resulted in the N-3 giving rise to a *N*-hydroxyurea (compound **20**). The use of this functional group as metal chelator in MMP inhibitors has been previously reported⁶ and recently validated by a X-ray structure.³¹

In order to determine the affinity of the *N*-hydroxyurea moiety, the model compound **15** was tested in silico and synthesized (see Scheme 3).

The in silico model suggested that the interaction of **15** with the active site is limited to the catalytic zinc and to the entrance into the S'_1 subsite. The structure of the adduct shows the same coordination scheme of the hydroxamic acid which is able both to chelate the active-site zinc ion and to provide a hydrogen bond interaction with the enzyme backbone. The protonated oxygen atom (O4) is involved in a strong hydrogen bond with carboxylate Oε2 of Glu219, while the NH shows weaker electrostatic interaction with the Ala181 carbonyl oxygen.

To determine the binding affinity for the MMP-12 catalytic domain, we analyzed the alteration of the chemical shifts induced on 2D ^1H - ^{15}N HSQC upon the titration with the *N*-hydroxyurea derivative **15**. The fit of the experimental data provided a dissociation constant of 3.4 mM. The binding mode predicted in silico is supported by the pattern of resonance frequencies shifted as a consequence of the interaction. The NH signal corresponding to His218 is strongly affected by millimolar concentration of the ligand (Fig. 3), while only few residues forming the S'_1 cavity are weakly influenced.

Since the metal binding capability of the *N*-hydroxyurea was confirmed, the new scaffold **20** was synthesized. (see Scheme 4)

The ^1H - ^{15}N HSQC spectra for **20** showed a pattern of shifts similar to compounds **9–12** indicating for all these molecules the same binding site (Fig. 4).

A different effect on the zinc binding histidine with respect to the *N*-hydroxyurea prototype is probably present since the shift perturbation involved mainly His222 instead of His218. The fit of $\Delta\delta$ as a function of the ligand concentration provided a K_D of 154 μM , in good agreement with the IC_{50} value of 149 μM obtained by the enzymatic assay (Fig. 4).

To probe the selectivity towards MMP-12, *N*-hydroxyurea **20** was also tested by fluorescence enzymatic experiments for the inhibition of collagenases (MMP-1,

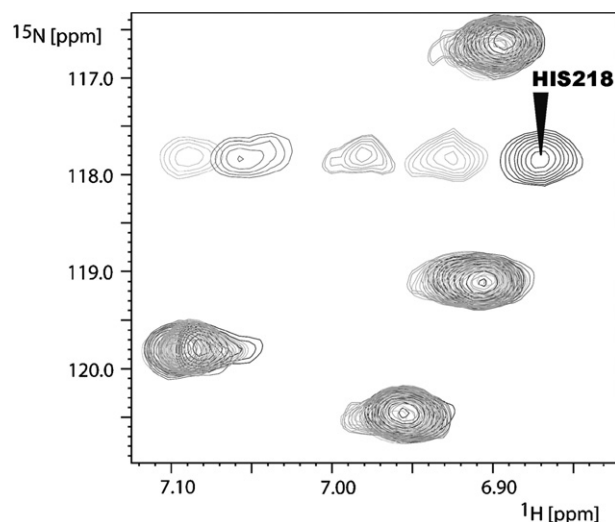


Figure 3. Expansion of ^1H - ^{15}N HSQC spectrum showing the shift of the His218 backbone NH upon the addition of increasing concentration of compound **15**.

MMP-8, MMP-13), matrilysin 1 (MMP-7) and stromelysin 2 (MMP-10) and the corresponding data are summarized in Table 2. Compound **20** is a fairly selective MMP-12 inhibitor since it possesses limited activity against the other MMPs especially the MMP-1 and MMP-7. These two enzymes differ from other MMP family members since they have a relatively small S'_1 pocket which presumably cannot accommodate the large biaryl substituent.

Although compound **20** exhibits an improved affinity towards MMP-12, nevertheless the micromolar value of K_D demonstrates that all the planned interactions are not optimized. The X-ray structure of the MMP-12-**20** complex (PDB code: 2HU6) provided a direct inspection on ligand-protein interactions (Fig. 5A). As correctly predicted by the NMR studies the molecule binds the metalloelastase at the catalytic site, fitting the biaryl moiety into the S'_1 pocket. The electron density of the inhibitor is well defined because it is held in place by two hydrogen bonds with Pro238 and Leu181 of the enzyme backbone. However, the contribution of the hydroxyurea to the binding is absolutely negligible since it points towards the exterior of the active site and does not interact with the catalytic zinc ion.

Noteworthy, the zinc ion is coordinated by the weak inhibitor acetohydroxamic acid (AHA) present, as stabilizer, in the crystallization buffer. This would suggest that the lack of interaction between the hydroxyurea and the catalytic zinc, evidenced in the crystal structure, is due to the competition with the high concentration of AHA.

In order to investigate this point, an energy minimization of the ligand was performed after removing AHA from the PDB and blocking the biaryl group in the crystal structure conformation. The AMBER-8 minimized model indicates that the hydroxyurea function could

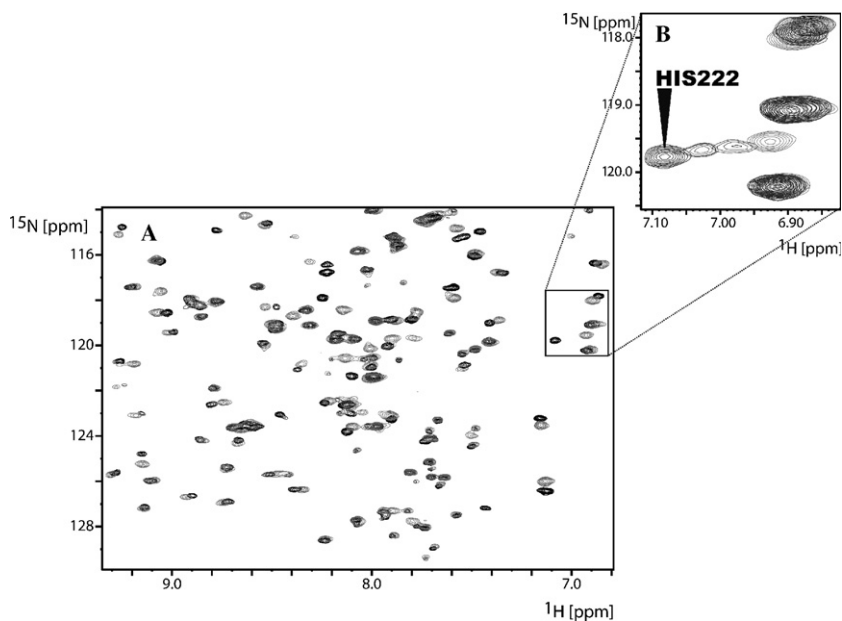


Figure 4. (A) ^1H - ^{15}N HSQC spectrum of MMP-12 catalytic domain in absence (black) and in presence (light grey) of compound **20** (500 μM). (B) Expansion of ^1H - ^{15}N HSQC spectrum showing the shift of the His222 backbone NH upon the addition of increasing concentration of compound **20**.

Table 2. MMP enzyme inhibition potency of compound **20** measured by enzymatic assay

Compound	IC_{50} (μM)					
	MMP-1	MMP-7	MMP-8	MMP-10	MMP-12	MMP-13
20	1180	1510	513	865	149	778

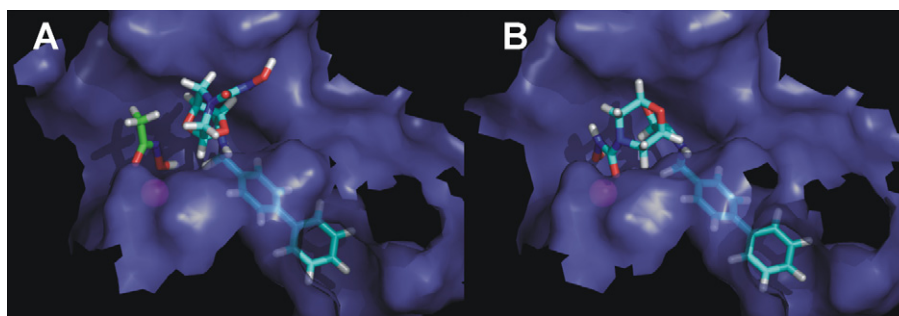


Figure 5. (A) Crystal structure of MMP-12-**20** adduct; the zinc ion is coordinated by AHA (Green). (B) AMBER-8-minimized model of MMP-12-**20** adduct.

coordinate the zinc ion, even if the hydrogen bond interactions with the zinc binding site are not well defined as in the case of AHA (Fig. 5B).

Therefore, these data suggest that the anchoring point and/or the length of the ZBG are not optimized and further studies have to be carried out in order to design a nanomolar inhibitor.

4. Conclusion

New compounds with affinity for the catalytic domain of the MMP-12 were designed using an integrated approach based on virtual screening and on NMR analysis. The molecules are built around a BTAa scaffold

fold functionalized with a biphenyl moiety and with a ZBG.

The adducts provided by docking calculation enabled the identification of the catalytic pocket of MMP-12 as the binding site for this class of compounds. The inspection of the residues showing a significant chemical shift perturbation supports this picture, with the lipophilic moiety fitted into S'_1 cavity and the bicyclic skeleton located outside, in front of the catalytic zinc.

Among the synthesized compounds, the scaffold **20** having the *N*-hydroxyurea group in position 3 and the *p*-phenylbenzylcarboxy amide in position 7 showed an improved affinity ($K_D = 154 \mu\text{M}$ and $\text{IC}_{50} 149 \mu\text{M}$) for MMP-12 and some selectivity towards the other MMPs.

The X-ray structure of the catalytic domain of Human Macrophage Metalloelastase in the presence of hydroxyurea derivative **20** gave more insight into the ligand–enzyme interaction and appeared as a new starting point for further MMP-12 inhibitors' designing.

New fragments may be easily inserted in the bicyclic scaffold to better interact with the enzyme backbone and to selectively accommodate into the binding pocket of MMP-12. Therefore, the synthetic versatility of BTAs, taken together with dissociation constant in micromolar range and fair selectivity, candidate these molecules as new compound guides to develop more potent and selective inhibitors for MMP-12.

5. Methods

Docking calculations were performed using the Lamarckian genetic algorithm (LGA) of the program Autodock 3.0³² which, using principles of natural evolution mutations and cross-over, probes the designed molecules on the three-dimensional structure of the target macromolecule. In this work, the crystal structure of the catalytic domain of MMP-12 (PDB code: 1RMZ), processed by AutoDockTools, was used as target protein. The three-dimensional structures of the designed ligands, generated by Chem3D Pro program, were minimized by semiempirical calculations and the Gasteiger–Marsili charges³³ assigned by the program Babel. In order to include all the active site, a box of $19.75 \times 19.75 \times 19.75 \text{ \AA}^3$, centred near the catalytic zinc and with a grid spacing of 0.275 \AA , was selected as docking space. A total of 50 runs were performed for each ligand and the results were ranked according to the docking energy.

The cDNA, encoding the fragment Gly106–Gly263 (F171D mutant)³⁴ of the macrophage metalloelastase, was cloned into the pET21 vector (Novagen) using *Nde*I and *Bam*HI as restriction enzymes and then transfected into *E. coli* strain BL21 Codon Plus cells. Uniform ¹⁵N-labelled protein was expressed by induction with 0.5 mM IPTG at $37 \text{ }^\circ\text{C}$ for 4 h in M9 minimal media containing 15 mM ($^{15}\text{NH}_4$)₂SO₄.

The inclusion bodies, containing the protein, were solubilized in a buffered solution with 20 mM Tris–HCl and 8 M urea at pH 8. The protein was then purified with a size-exclusion chromatography (Pharmacia HiLoad Superdex 75 16/60) in 6 M urea and 50 mM sodium acetate. A second step of purification was performed on cation exchange column Mono-S (Pharmacia) using a linear gradient of NaCl up to 0.5 M .

The protein was refolded by using a multi-step dialysis against solution containing 50 mM Tris–HCl (pH 7.2), 10 mM CaCl₂, 0.1 mM ZnCl₂, 0.3 M NaCl and decreasing concentrations of urea (from 4 M up to 2 M). The last two dialyses were performed against solution containing 20 mM Tris–HCl (pH 7.2), 5 mM CaCl₂, 0.1 mM ZnCl₂, 0.3 M NaCl and 200 mM of hydroxamic acid (AHA). The catalytic domains of

MMP-1 (Val101–Pro269), MMP-7 (Tyr100–Lys272), MMP-8 (Met100–Gly262), MMP-10 (Phe99–Gly263, F170N mutant), MMP-13 (Tyr104–Pro269) were expressed, purified and refolded according to the protocol already described for MMP-12, with minor modifications.

¹H–¹⁵N HSQC experiments, implemented with the sensitivity enhancement scheme,³⁵ were recorded at 298 K on a Bruker DRX 700 operating at proton nominal frequency of 700.21 MHz . The NMR experiments were performed on samples containing 0.1 mM of ¹⁵N-enriched MMP-12 in 10 mM Tris–HCl buffer, 10 mM CaCl₂, 0.1 mM ZnCl₂, 0.3 M NaCl and 0.2 M acetohydroxamic acid at pH 7.2.

The compounds were evaluated for their ability to inhibit the hydrolysis of fluorescence-quenched peptide substrate Mca-Pro-Leu-Gly-Leu-Dpa-Ala-Arg-NH₂ (Biomol, Inc.). The assays were performed in 50 mM HEPES buffer, containing 10 mM CaCl₂, 0.05% Brij-35, at pH 7, using 1 nM of proteolytic enzyme (catalytic domains of MMP-1, MMP-7, MMP-8, MMP-10, MMP-12, MMP-13) and $1 \text{ } \mu\text{M}$ of peptide. The enzyme was incubated at $25 \text{ }^\circ\text{C}$ with increasing concentration of inhibitor and the fluorescence (excitation_{max} 328 nm ; emission_{max} 393 nm) was measured for 3 min after the addition of the substrate using a Varian Eclipse fluorimeter. Fitting of rates as a function of inhibitor concentration provided IC₅₀ values (see Table 1). The inhibitor *N*-isobutyl-*N*-[4-methoxyphenylsulfonyl]glycyl hydroxamic acid (Biomol, Inc.) was used as control.

Crystals of human MMP-12, already containing AHA from the refolding process, grew at $20 \text{ }^\circ\text{C}$ from a 0.1 M Tris–HCl, 30% PEG 6000, 200 mM AHA, 1.0 M LiCl₂ solution at pH 8.0 using the vapour diffusion technique. The final protein concentration was about 10 mg/ml . Soaking procedure was implemented in order to allow the inhibitor binding; **20** was added in the powdered form directly into the drop using a needle and was left incubating for a few days. The data were measured exploiting synchrotron radiation at the beamline ID23-1 (ESRF, Grenoble, France). The dataset was collected at 100 K and the crystal used for data collection was cryo-cooled without any cryo-protectant treatment. The crystal diffracted up to 1.3 \AA resolution and belongs to space group *C*2 ($a = 51.25 \text{ \AA}$, $b = 60.18 \text{ \AA}$, $c = 53.97 \text{ \AA}$, $\alpha = \gamma = 90^\circ$, $\beta = 114.59^\circ$) with one molecule in the asymmetric unit, a solvent content of about 50% and a mosaicity of 0.7° . The data were processed in all cases using the program MOSFLM³⁶ and scaled using the program SCALA³⁷ with the TAILS and SECONDARY corrections on (the latter restrained with a TIE SURFACE command) to achieve an empirical absorption correction.

Table 3 shows the data collection and processing statistics for all datasets. The structure was solved using the molecular replacement technique; the model used was that of the MMP-12–AHA adduct (1Y93) from where the inhibitor, all the water molecules and ions were

Table 3. Data collection and anisotropic refinement statistics^a

Space group	C2
Cell dimensions (Å, °)	$A = 51.25, b = 60.18,$ $c = 53.97, \beta = 114.59$
Resolution (Å)	49.10–1.32
Unique reflections	34825 (5291)
Overall completeness (%)	99.0 (98.8)
$R_{\text{sym}}(\%)$	5.3 (27.6)
Multiplicity	3.1 (2.9)
$I/(\sigma I)$	8.6 (2.5)
Wilson plot B -factor (Å ²)	10.55
$R_{\text{cryst}}/R_{\text{free}}$ (%)	16.2/18.7
Protein atoms (excluding hydrogens)	1238
Ions	5
Ligand atoms	33
Water molecules	300
rmsd bond lengths (Å)	0.006
rmsd bond angles (°)	1.0
Mean B -factor (Å ²)	13.90

^a The numbers in parentheses refer to values in the highest resolution shell.

omitted. The correct orientation and translation of the molecule within the crystallographic unit cell was determined with standard Patterson search techniques^{38,39} as implemented in the program MOLREP.^{40,41} The anisotropic refinement was carried out using REFMAC5.⁴² In between the refinement cycles the model was subjected to manual rebuilding by using XtalView.⁴³ The same program was used to model the inhibitors. Water molecules were added by using the standard procedures within the ARP/WARP suite.⁴⁴ The stereochemical quality of the refined models was assessed using the program Procheck.⁴⁵ The Ramachandran plot is of very good quality.

6. Experimental

Melting points are uncorrected and were measured on microscope RCH Kofler apparatus. Chromatographic purifications were recorded with silica gel 60 (0.040–0.063 mm), unless otherwise stated, using flash column techniques; all TLC development was performed on silica gel coated (Merck Silica gel 60 F₂₅₄, 0.25 mm) sheets. IR spectra were recorded on Perkin-Elmer 881 spectrophotometer. ¹H and ¹³C NMR spectral analyses were obtained on a Varian Gemini 200 (200 MHz for ¹H and 50.33 MHz for ¹³C) instrument or a Varian Mercury 400 (400 MHz for ¹H and 100 MHz for ¹³C) instrument using tetramethylsilane as internal standard and the chemical shifts were reported in δ (ppm) units. EI mass spectral analyses were carried out at 70 eV ionizing voltage by direct introduction on a QMD 1000 Carlo Erba instrument, whereas ESI-MS spectra were carried out on LTQ Thermo Finnigan instrument. Microanalyses were carried out on Perkin Elmer 240 C elemental analyser. Optical rotation measurements were performed on JASCO DIP-370 digital polarimeter. All reactions requiring anhydrous conditions were carried out under N₂ atmosphere and were performed in oven-dried glassware.

Preparation of acid silica gel (SiO₂/H₂SO₄): SiO₂ (29 g) was suspended in CH₂Cl₂ (400 ml) with 12 g of H₂SO₄ and left under vigorous magnetic stirring for 40 min. The suspension was then concentrated at low pressure.

6.1. Biphenyl-4-yl-methyl-(2,2-dimethoxy-ethyl)-amine (3)

A solution containing 2,2-dimethoxy-ethylamine (14.4 g, 137 mmol) and biphenyl-4-carbaldehyde (25 g, 137 mmol) in MeOH (300 ml) was stirred at room temperature for 2.5 h. NaBH₄ was then slowly added at 0 °C and the reaction mixture was stirred at room temperature overnight. Once the reaction was completed MeOH was evaporated in vacuo and the crude residue was suspended in ethyl acetate, washed with water and dried over Na₂SO₄. The resulting product was used in next step without further purification. Purification by column chromatography using ethyl acetate/petroleum ether (1:1) as eluent afforded the pure **3** as a colourless oil.

¹H NMR (CDCl₃): δ 7.62–7.26 (m, 9H), 4.53 (t, 1H, $J = 5.5$ Hz), 3.86 (s, 2H), 3.39 (s, 6H), 2.80 (d, 2H, $J = 5.6$ Hz); ¹³C (CDCl₃): δ 140.9, 139.9, 139.1 (s), 128.7–127.0 (d), 104.0 (d), 54.10 (t), 53.68 (t), 50.70 (q); MS m/z 271 (M⁺, 15), 167 (100); IR (CHCl₃) 3323, 2829 cm⁻¹; Anal. Calcd for C₁₆H₁₉NO₂ (257.1): C, 74.68; H, 7.44; N, 5.44. Found: C, 74.75; H, 7.52; N, 5.65.

6.2. (2*R*,6*R*/*S*)-(4-Biphenyl-4-yl-methyl-6-methoxy-3-oxo-morpholin-2-yl)-(R)-hydroxyacetic acid methyl ester (6)

To a suspension of (*R,R*)-2,3-di-*O*-acetyltartaric anhydride (**4**) (30 g, 137 mmol) in dry DCM (120 ml) was added, at 0 °C and under N₂ atmosphere, a solution of **3** (37 g, 137 mmol) in dry DCM (60 ml). The reaction mixture was stirred at room temperature overnight. After evaporation of the solvent, the crude product was dissolved in MeOH (230 ml) and thionyl chloride (8.5 ml, 116 mmol) was added dropwise at 0 °C. The mixture was then allowed to reach 60 °C and stirred for 2 h. The solvent was removed and the crude product was isolated as a yellow oil and used without further purification in the next step. Purification of the crude product by column chromatography (ethyl acetate/petroleum ether 2:1) afforded **6** as a white solid.

Mp 115–120 °C; $[\alpha]_{\text{D}}^{26} +111.1$ (c 1.3, CHCl₃); ¹H NMR (CDCl₃): δ 7.60–7.26 (m, 9H), 4.96 (s, 1H), 4.87 (s, 1H), 4.84 (d, 1H, $J = 14$ Hz), 4.64 (s, 1H), 4.54 (d, 1H, $J = 14$ Hz), 3.85 (s, 3H), 3.58 (dd, 1H, $J_1 = 14$ Hz, $J_2 = 3.2$ Hz), 3.39 (s, 3H), 3.16 (d, 1H, $J = 14$ Hz); ¹³C NMR (CDCl₃): δ 172.4 (s), 165.4 (s), 140.6, 140.4, 134.5 (s), 128.7, 128.2, 127.4, 127.2, 127.0 (d), 95.95 (d), 72.28 (d), 71.60 (d), 55.15 (q), 52.89 (q), 49.65 (t), 49.55 (t); MS m/z 385 (M⁺, 58), 167 (100); IR (CHCl₃) 3545, 1745, 1654 cm⁻¹; Anal. Calcd for C₂₁H₂₃NO₆ (385.2): C, 65.44; H, 6.02; N, 3.63. Found: C, 65.03; H, 6.22; N, 3.27.

6.3. (1*S*,5*S*,7*R*)-3-Biphenyl-4-ylmethyl-2-oxo-3-aza-6,8-dioxo-bicyclo[3.2.1]octane-7-carboxylic acid methyl ester (7)

A solution of **6** (52 g, 137 mmol) in toluene (200 ml) was quickly added to a refluxing suspension of H₂SO₄/SiO₂ (29 g) in toluene (400 ml). The mixture was allowed to react for 20 min and one-third of the solvent was distilled off. The hot reaction mixture was filtered through a short layer of NaHCO₃ and, after evaporation of the solvent, the crude product was purified by column chromatography using ethyl acetate/petroleum ether (2:1) as eluent and affording **7** (20 g, 41% over four steps) as a white solid.

Mp 160–165 °C; $[\alpha]_D^{25}$ –40.5 (*c* 1.0, CHCl₃); ¹H NMR (CDCl₃): δ 7.60–7.26 (m, 9H), 5.89 (d, 1H, *J* = 2.2 Hz), 5.01 (s, 1H), 4.79 (s, 1H), 4.66–4.52 (AB system, 2H), 3.81 (s, 3H), 3.42 (dd, 1H, *J*₁ = 2.2 Hz, *J*₂ = 12 Hz), 3.17 (d, 1H, *J* = 12 Hz); ¹³C NMR (CDCl₃): δ 169.0 (s), 165.4 (s), 140.9, 140.4, 134.2 (s), 128.7, 128.4, 127.6, 127.4, 127.0 (d), 100.1 (d), 77.83 (d), 77.73 (d), 52.93 (q), 51.23 (t), 48.21 (t); MS *m/z* 353 (M⁺, 11), 167 (100); IR (CHCl₃) 1756, 1674 cm⁻¹; Anal. Calcd for C₂₀H₁₉NO₅ (353.1): C, 67.98; H, 5.42; N, 3.96. Found: C, 67.54; H, 5.42; N, 3.69.

6.4. (1*S*,5*S*,7*R*)-3-Biphenyl-4-ylmethyl-3-aza-6,8-dioxo-bicyclo[3.2.1]octane-7-carboxylic acid methyl ester (8)

BH₃·SMe₂ (0.403 ml, 4.2 mmol) was added dropwise to a cooled (0 °C) solution of **7** (1 g, 2.8 mmol) in dry THF under N₂ atmosphere and the resulting mixture was stirred at room temperature overnight. Once the reaction was completed EtOH (2 ml) and H₂O were added and the resulting mixture was washed with OEt₂. The organic layer was dried over Na₂SO₄ and concentrated in vacuo. The crude product was purified by column chromatography using ethyl acetate/petroleum ether (3:1) as eluent to afford **8** (670 mg, 70%) as a white solid.

Mp 130–134 °C; $[\alpha]_D^{24}$ –57.0 (*c* 1.0, CHCl₃); ¹H NMR (CDCl₃): δ 7.63–7.36 (m, 9H), 5.66 (s, 1H), 4.86 (s, 1H), 4.66 (s, 1H), 3.78 (s, 3H), 3.70–3.50 (AB system, 2H), 2.87 (pseudo t, 2H, *J* = 11.6 Hz), 2.56 (dd, 1H, *J*₁ = 1.6, *J*₂ = 11.2 Hz), 2.35 (d, 1H, *J* = 12 Hz); ¹³C NMR (CDCl₃): δ 171.4 (s), 140.7, 140.2, 136.3 (s), 129.2, 128.7, 127.2, 127.1, 127.0 (d), 101.4 (d), 77.00 (d), 76.07 (d), 61.16 (t), 56.44 (t), 54.85 (t), 52.54 (q); MS *m/z* 339 (M⁺, 23), 167 (100); IR (CHCl₃) 1753, 1733 cm⁻¹; Anal. Calcd for C₂₀H₂₁NO₄ (339.2): C, 70.78; H, 6.24; N, 4.13. Found: C, 70.34; H, 6.41; N, 4.00.

6.5. (1*S*,5*S*,7*R*)-3-Biphenyl-4-ylmethyl-2-oxo-3-aza-6,8-dioxo-bicyclo[3.2.1]octane-7-carboxylic acid (9)

A solution containing **7** (85 mg, 0.24 mmol) and LiOH (25 mg, 0.6 mmol) in a mixture of MeOH and THF in a 2:1 ratio (5 ml) was stirred overnight at room temperature. The reaction mixture was then acidified with 5% HCl and the organic solvents were removed in vacuo. The remaining aqueous layer was washed with DCM

and the resulting organic phase was dried over Na₂SO₄ and concentrated under reduced pressure to afford **9** (65 mg, 80%) as a white solid.

Mp 186–195 °C; ¹H NMR (DMSO): δ 7.66–7.27 (m, 9H), 5.95 (s, 1H), 4.89 (s, 1H), 4.80 (s, 1H), 4.60–4.42 (AB system, 2H), 3.38 (d, 1H, *J* = 14 Hz), 3.10 (d, 1H, *J* = 14); ¹³C NMR (DMSO): δ 170.6 (s), 165.7 (s), 140.1, 139.7, 135.9 (s), 129.3, 128.7, 127.8, 127.4, 127.0 (d), 99.85 (d), 77.62 (d), 77.50 (d), 51.64 (t), 47.39 (t); MS *m/z* 339 (M⁺, 17), 167 (100); Anal. Calcd for C₁₉H₁₇NO₅ (339.1): C, 67.25; H, 5.05; N, 4.13. Found: C, 66.86; H, 5.06; N, 4.04.

6.6. (1*S*,5*S*,7*R*)-3-Biphenyl-4-ylmethyl-3-aza-6,8-dioxo-bicyclo[3.2.1]octane-7-carboxylic acid (10)

A solution containing **8** (80 mg, 0.23 mmol) and aq. HCl 4 M (0.800 ml) was stirred overnight at room temperature. The product was then freeze-dried affording **10** (75 mg, 90%) as a white solid.

Mp 158–165 °C; ¹H NMR (DMSO): δ 11.18 (br s, 1H), 7.72–7.67 (m, 5H), 7.48–7.35 (m, 4H), 5.83 (s, 1H), 5.45 (s, 1H), 4.97 (s, 1H), 4.34 (m, 2H), 3.60–3.48 (m, 1H), 3.42–3.22 (m, 1H), 3.20–2.96 (m, 2H); ¹³C NMR (DMSO) (carboxylic carbon not detected): δ 139.7, 132.8 (s), 129.4–127.1 (d), 101.0 (d), 75.03 (d), 74.31 (d), 59.47 (t), 53.19 (t), 52.86 (t); MS *m/z* 325 (M⁺, 21), 167 (100); IR (KBr) 3406, 2355, 1741 cm⁻¹; Anal. Calcd for C₁₉H₂₀ClNO₄ (361.11): C, 63.07; H, 5.57; N, 3.87. Found: C, 62.88; H, 5.71; N, 3.75.

6.7. (1*S*,5*S*,7*R*)-3-Biphenyl-4-ylmethyl-2-oxo-3-aza-6,8-dioxo-bicyclo[3.2.1]octane-7-carboxylic acid hydroxyamide (11)

A solution containing **7** (100 mg, 0.28 mmol), hydroxylamine hydrochloride (97 mg, 1.42 mmol) and NEt₃ (236 μl, 1.7 mmol) in CHCl₃ (500 μl) was stirred for 5 days at room temperature. The resulting suspension was then filtered and the organic solvents were evaporated in vacuo. The crude product was purified by column chromatography, using ethyl acetate as eluent and affording **11** (21 mg, 21%) as a white solid.

Mp 197–203 °C; ¹H NMR (DMSO): δ 10.74 (br s, 1H), 9.00 (br s, 1H), 7.71–7.17 (m, 9H), 5.92 (s, 1H), 4.69 (s, 2H), 4.49 (s, 2H), 3.39 (d, 1H, *J* = 12 Hz), 3.07 (d, 1H, *J* = 12 Hz); ¹³C NMR (DMSO): δ 165.9 (s), 165.2 (s), 140.1, 139.7, 135.9 (s), 129.3, 128.7, 127.8, 127.4, 127.0 (d), 99.84 (d), 78.84 (d), 77.46 (d), 51.60 (t), 47.41 (t); MS *m/z* 354 (M⁺, 2), 167 (100); Anal. Calcd for C₁₉H₁₈N₂O₅ (354.1): C, 64.40; H, 5.12; N, 7.91. Found: C, 64.12; H, 5.42; N, 7.53.

6.8. (1*S*,5*S*,7*R*)-3-Biphenyl-4-ylmethyl-3-aza-6,8-dioxo-bicyclo[3.2.1]octane-7-carboxylic acid hydroxyamide (12)

A solution containing **8** (98 mg, 0.29 mmol), hydroxylamine hydrochloride (97 mg, 1.42 mmol) and NEt₃ (242 μl, 1.7 mmol) in CHCl₃ (500 μl) was stirred for 5 days at room temperature. The resulting suspension

was then filtered and the organic solvents were evaporated in vacuo. The crude product was purified by column chromatography, using ethyl acetate as eluent, affording **12** (26 mg, 26%) as a white solid.

Mp 185–189 °C; ¹H NMR (DMSO): δ 10.55 (s, 1H), 8.80 (s, 1H), 7.67–7.34 (m, 9H), 5.56 (s, 1H), 4.52 (s, 1H), 4.46 (s, 1H), 3.56 (s, 2H), 2.75 (pseudo t, 2H, *J* = 10 Hz), 2.42 (d, 1H, *J* = 11.4 Hz), 2.18 (d, 1H, *J* = 11.6 Hz); ¹³C NMR (DMSO): δ 167.3 (s), 140.3, 137.1 (s), 129.7, 129.3, 129.2, 127.7, 127.0 (d), 100.5 (d), 76.92 (d), 76.73 (d), 60.66 (t), 56.42 (t), 55.28 (t); ESI MS *m/z* 341 (M+1); IR (KBr) 3317, 3146, 1683 cm⁻¹; Anal. Calcd for C₁₉H₂₀N₂O₄ (340.1): C, 67.05; H, 5.92; N, 8.23. Found: C, 66.66; H, 5.45; N, 8.61.

6.9. 1-Benzoyloxycarbonyl-piperidine-4-carboxylic acid ethyl ester (**14**)

A solution of piperidine-4-carboxylic acid ethyl ester (**13**) (300 mg, 1.91 mmol) in dry DCM (5 ml) was added to a solution of triphosgene (187 mg, 0.63 mmol) in dry DCM (4 ml) at 0 °C and under inert atmosphere. The resulting solution was allowed to reach room temperature and stirred for 1 day.

To the reaction mixture were then added *O*-benzyl-hydroxylamine hydrochloride (336 mg, 2.1 mmol) and NEt₃ (850 μl, 6.1 mmol) and the resulting solution was stirred for 2 h. The reaction mixture was then concentrated under reduced pressure, diluted with DCM, washed with H₂O and brine, dried over Na₂SO₄ and concentrated in vacuo. The crude product was purified by column chromatography (Aluminium oxide, ethyl acetate/petroleum ether 2:1 to clean up impurities; ethyl acetate to isolate the final product) to afford **14** (238 mg, 40%) as a pale yellow oil.

¹H NMR (CDCl₃): δ 7.54–7.25 (br s, 5H), 7.11 (br s, 1H), 4.84 (s, 2H), 4.14 (q, 2H, *J* = 7.07 Hz), 3.95–3.78 (m, 2H), 3.02–2.79 (m, 2H), 2.57–2.35 (m, 1H), 1.99–1.80 (m, 2H), 1.77–1.51 (m, 2H), 1.25 (t, 3H, *J* = 7.11 Hz); ¹³C NMR (CDCl₃): δ 174.2 (s), 158.8 (s), 135.9 (s), 129.1, 128.5, 128.5 (d), 77.94 (t), 60.61 (t), 43.32 (t), 40.79 (d), 27.70 (t), 14.17 (q); MS *m/z* 306 (M⁺, 1), 91 (100); IR (CHCl₃) 1724, 1676, 1222 cm⁻¹; Anal. Calcd for C₁₆H₂₂N₂O₄ (306.16): C, 62.73; H, 7.24; N, 9.14. Found: C, 61.65; H, 7.74; N, 8.94.

6.10. 1-Hydroxycarbonyl-piperidine-4-carboxylic acid ethyl ester (**15**)

A stirred solution of **14** (150 mg, 0.5 mmol) in AcOEt was submitted to hydrogenolysis over 10% Pd/C at 1 atm overnight. After separation of the catalyst by centrifugation, the solvent was evaporated and the crude residue washed with Et₂O affording **15** (108 mg, quantitative) as a white solid.

Mp 101–104 °C; ¹H NMR (CDCl₃): δ 6.46 (br s, 1H), 4.13 (q, 2H, *J* = 7.09 Hz), 3.86 (dt, 2H, *J*₁ = 13.45, *J*₂ = 3.69 Hz), 3.05–2.81 (m, 2H), 2.48 (m, 1H),

2.03–1.82 (m, 2H), 1.78–1.53 (m, 2H), 1.24 (t, 3H, *J* = 7.16); ¹³C NMR (CDCl₃): δ 171.8 (s), 158.2 (s), 58.02 (t), 40.14 (t), 37.91 (d), 24.81 (t), 11.44 (q); ESI MS *m/z* 217 (M+1); IR (CHCl₃) 3682, 1724, 1668, 1218 cm⁻¹; Anal. Calcd for C₉H₁₆N₂O₄ (216.11): C, 49.99; H, 7.46; N, 12.96. Found: C, 49.55; H, 7.45; N, 12.89.

6.11. (1*S*,5*S*,7*R*)-3-Benzyl-3-aza-6,8-dioxo-bicyclo[3.2.1]octane-7-carboxylic acid (biphenyl-4-ylmethyl)-amide (**17**)

A mixture containing BnBTGOMe (**16**) (314 mg, 1.19 mmol) and biphenyl-4-yl-methylamine (1 g, 4.6 mmol) was allowed to reach 60 °C and was stirred at the same temperature overnight. Once the reaction was completed the crude product was purified by column chromatography using ethyl acetate/petroleum ether (1:2) as eluent and affording **17** (460 mg, 93%) as a white solid.

Mp 98–101 °C; [α]_D²³ +23.7 (*c* 0.5, CH₂Cl₂); ¹H NMR (CDCl₃): δ 7.58–7.19 (m, 14H), 6.97 (br s, 1H), 5.59 (s, 1H), 4.79 (s, 1H), 4.69 (s, 1H), 4.65–4.37 (m (ABX system), 2H), 3.57 (m, 2H), 2.87 (d, 2H, *J* = 10.6 Hz), 2.55 (d, 1H, *J* = 11.8 Hz), 2.34 (d, 1H, *J* = 11 Hz); ¹³C NMR (CDCl₃): δ 171.1 (s), 140.6, 140.4, 136.7 (s), 128.8, 128.7, 128.4, 128.0, 127.4, 127.3, 127.3, 127.0 (d), 101.2 (d), 77.44 (d), 77.38 (d), 61.54 (t), 56.30 (t), 55.02 (t), 42.87 (t); MS *m/z* 414 (M⁺, 7), 91 (100); IR (CHCl₃) 3418, 1674, 1521, 1106 cm⁻¹; Anal. Calcd for C₂₆H₂₆N₂O₃ (414.19): C, 75.34; H, 6.32; N, 6.76. Found: C, 74.96; H, 6.25; N, 6.37.

6.12. (1*S*,5*S*,7*R*)-3-Aza-6,8-dioxo-bicyclo[3.2.1]octane-7-carboxylic acid (biphenyl-4-ylmethyl)-amide (**18**)

A solution of **17** (438 mg, 1.06 mmol) and ammonium formate (300 mg, 4.76 mmol) in MeOH (8 ml) and over 10% Pd/C was refluxed for 2 h under N₂ atmosphere. After separation of the catalyst by filtration over a pad of Celite, the solvent was evaporated to afford **18** (220 mg, 64%) as a white solid.

Mp 89–92 °C; [α]_D²² +11.8 (*c* 1.0, CHCl₃); ¹H NMR (CDCl₃): δ 7.59–7.26 (m, 9H), 6.98 (br s, 1H), 5.57 (s, 1H), 4.79 (s, 1H), 4.68 (s, 1H), 4.52 (m, 2H), 3.29 (d, 1H, *J* = 13.2 Hz), 2.98 (d, 2H, *J* = 13.6 Hz), 2.80 (d, 1H, *J* = 13.6 Hz); ¹³C NMR (CDCl₃): δ 171.0 (s), 140.6, 136.7 (s), 128.7, 128.0, 127.4, 127.3, 127.0 (d), 101.1 (d), 77.42 (d), 54.21 (t), 53.84 (t), 42.86 (t); MS *m/z* 324 (M⁺, 5), 167 (100); IR (CHCl₃) 3420, 1673, 1527, 1110 cm⁻¹; Anal. Calcd for C₁₉H₂₀N₂O₃ (324.15): C, 70.35; H, 6.21; N, 8.64. Found: C, 70.25; H, 5.91; N, 8.90.

6.13. (1*S*,5*S*,7*R*)-3-Aza-6,8-dioxo-bicyclo[3.2.1]octane-3,7-dicarboxylic acid 3-(benzyloxy-amide) 7-[(biphenyl-4-ylmethyl)-amide] (**19**)

O-Benzyl-hydroxylamine¹⁶ (69 mg, 0.56 mmol) was dissolved in anhydrous THF (1.6 ml) and added dropwise to a cooled solution of carbonyldiimidazole (91 mg,

0.56 mmol) in 5 ml of dry THF under N₂ atmosphere. After being stirred for 30 min at room temperature, the resulting solution was added to the neat **18** (181 mg, 0.56 mmol) and the reaction mixture was stirred overnight. The solution was then diluted with AcOEt, washed with water and brine, dried over Na₂SO₄ and evaporated in vacuo. Crystallization at room temperature from ethyl acetate afforded the pure **19** (160 mg, 60%) as a white solid.

Mp 110–114 °C; $[\alpha]_D^{26} +29.6$ (*c* 0.77, CDCl₃); ¹H NMR (CDCl₃): δ 7.60–7.26 (m, 14H), 6.90 (br s, 1H), 5.62 (s, 1H), 4.85 (s, 2H), 4.76 (s, 1H), 4.60–4.48 (m, 3H), 3.89 (d, 1H, *J* = 12.8 Hz), 3.70 (d, 1H, *J* = 12.8 Hz), 3.33 (d, 1H, *J* = 13 Hz), 3.04 (d, 1H, *J* = 12.8 Hz); ¹³C NMR (CDCl₃): δ 169.9 (s), 159.3 (s), 140.6, 136.4, 135.5 (s), 129.0, 128.7, 128.5, 128.5, 128.0, 127.4, 127.4, 127.0 (d), 99.78 (d), 78.21 (d), 75.69 (d), 47.42 (t), 46.88 (t), 42.98 (t); MS *m/z* 473 (M⁺, 2), 324 (12), 167 (100), 91 (61); IR (CDCl₃) 3420, 1677, 1527 cm⁻¹; Anal. Calcd for C₂₇H₂₇N₃O₅ (473.20): C, 68.48; H, 5.75; N, 8.87. Found: C, 68.38; H, 5.61; N, 8.92.

6.14. (1*S*,5*S*,7*R*)-3-Aza-6,8-dioxa-bicyclo[3.2.1]octane-3,7-dicarboxylic acid 7-[(biphenyl-4-ylmethyl)-amide] 3-hydroxyamide (**20**)

A stirred solution of **19** (120 mg, 0.25 mmol) in THF was submitted to hydrogenolysis over 10% Pd/C at 1 atm, at room temperature, overnight. After separation of the catalyst by filtration through a pad of Celite, the solvent was evaporated and the crude residue washed with Et₂O affording **20** (65 mg, 68%) as a white solid.

Mp 75–80 °C; $[\alpha]_D^{26} +36.6$ (*c* 0.75, CDCl₃); ¹H NMR (CDCl₃): (Mixture of rotamers): δ 11.58 (br s, 1H), 8.41 (br s, 1H), 7.62–7.20 (m, 9H), 7.13–6.90 (m, 1H), 5.65 (s, 1H, minor rotamer), 5.60 (s, 1H, major rotamer), 4.78 (s, 1H, minor rotamer), 4.73 (s, 1H, major rotamer), 4.66–4.57 (m, 1H), 4.55–4.38 (m, 2H), 4.02–3.84 (m, 1H), 3.80–3.62 (m, 1H), 3.41–3.24 (m, 1H), 3.18–2.96 (m, 1H); ¹³C NMR (CDCl₃): (mixture of rotamers): δ 170.8 (s, major rotamer), 170.5 (s, minor rotamer), 161.5 (s, major r.), 159.0 (s, minor r.), 140.6, 140.5, 136.5 (s), 128.8–127.0 (d), 99.79 (d), 77.22 (d, minor r.), 76.93 (d, major r.), 75.68 (d), 47.46 (t, minor r.), 46.97 (t, major r.), 46.48 (t, minor r.), 45.88 (t, major r.), 42.80 (t); MS *m/z* 383 (M⁺, 0.2), 324 (7), 167 (100); IR (CDCl₃) 3420, 1668 cm⁻¹; Anal. Calcd for C₂₀H₂₁N₃O₅ (383.15): C, 62.65; H, 5.52; N, 10.96. Found: C, 62.30; H, 5.96; N, 10.40.

Acknowledgments

The authors thank Ministero della Ricerca Scientifica e Tecnologica, Roma; MIUR for contracts RBNE01TTJW, COFIN 2003–2005 and COFIN 2004–2006. GenExpress (Università di Firenze), Ente Cassa di Risparmio di Firenze, Marie Curie Training Sites (HPMT-CT-2000-00137) and CINMPIS are also acknowledged for financial support. C. M. thanks CERM for a PhD fellowship. The authors also thank

Mrs. B. Innocenti and Mr. M. Passaponti for technical assistance.

References and notes

1. Visse, R.; Nagase, H. *Circ. Res.* **2003**, *92*, 827–839.
2. Mandal, M.; Mandal, A.; Das, S.; Chakraborti, T.; Sajal, C. *Mol. Cell. Biochem.* **2003**, *252*, 305–329.
3. Whittaker, M.; Floyd, C. D.; Brown, P.; Gearing, A. J. *Chem. Rev.* **1999**, *99*, 2735–2776.
4. Skiles, J. W.; Gonnella, N. C.; Jeng, A. Y. *Curr. Med. Chem.* **2004**, *11*, 2911–2977.
5. Fisher, J. F.; Mobashery, S. *Cancer Metastasis Rev.* **2006**, *25*, 115–136.
6. Summers, J. B.; Gunn, B. P.; Mazdiyasi, H.; Goetz, A. M.; Young, P. R.; Bouska, J. B.; Dyer, R. D.; Brooks, D. W.; Carter, G. W. *J. Med. Chem.* **1987**, *30*, 2121–2126.
7. Michaelides, M. R.; Dellaria, J. F.; Gong, J.; Holms, J. H.; Bouska, J. J.; Stacey, J.; Wada, C. K.; Heyman, H. R.; Curtin, M. L.; Guo, Y.; Goodfellow, C. L.; Elmore, I. B.; Albert, D. H.; Magoc, T. J.; Marcotte, P. A.; Morgan, D. W.; Davidsen, S. K. *Bioorg. Med. Chem. Lett.* **2001**, *11*, 1553–1556.
8. Breuer, E.; Frant, J.; Reich, R. *Expert Opin. Ther. Patents* **2005**, *15*, 253–269.
9. Lukacova, V.; Zhang, Y. F.; Mackov, M.; Baricic, P.; Raha, S.; Calvo, J. A.; Balaz, S. *J. Biol. Chem.* **2004**, *279*, 14194–14200.
10. Coussens, L. M.; Fingleton, B.; Matrisian, L. M. *Science* **2002**, *295*, 2387–2392.
11. Pavlaki, M.; Zucker, S. *Cancer Metastasis Rev.* **2003**, *22*, 177–203.
12. Borkakoti, N. *Biochem. Soc. Trans.* **2004**, *32*, 17–20.
13. Fragai, M.; Nativi, C.; Richichi, B.; Venturi, C. *Chem-BioChem* **2005**, *6*, 1345–1349.
14. Hanessian, M.; Mackay, D. B.; Moitessier, N. *J. Med. Chem.* **2001**, *44*, 3066–3073.
15. (a) Guarna, A.; Guidi, A.; Machetti, F.; Menchi, G.; Occhiato, E. G.; Scarpi, D.; Sisi, S.; Trabocchi, A. *J. Org. Chem.* **1999**, *64*, 7347–7364; (b) Trabocchi, A.; Menchi, G.; Guarna, F.; Machetti, F.; Scarpi, D.; Guarna, A. *Synlett* **2006**, 331–353.
16. Trabocchi, A.; Mancini, F.; Menchi, G.; Guarna, A. *Mol. Diversity* **2003**, *6*, 245–250.
17. Klebe, G.; Gräder, U.; Grünemberg, S.; Krämer, O.; Gohlke, O.; *Understanding Receptor–Ligand Interaction as a Prerequisite for Virtual Screening*. In *Virtual Screening for Bioactive Molecules*, H. J. Böhm, G. Schneider, Eds.; Wiley–WCH, Weinheim, Germany, 2000; pp 207–227.
18. Lucas, H. J.; Baumgarten, W. *J. Am. Chem. Soc.* **1941**, *63*, 1653–1657.
19. Machetti, F.; Bucelli, I.; Indiani, G.; Guarna, A. *Chimie* **2003**, *6*, 631–633.
20. Defoin, A.; Brouillard-Poichet, A.; Streith, J. *Helv. Chim. Acta* **1992**, *75*, 109–123.
21. Romine, J. L.; Martin, S. W.; Meanwell, N. A.; Epperson, J. R. *Synthesis* **1994**, *8*, 846–850.
22. Bertini, I.; Calderone, V.; Cosenza, M.; Fragai, M.; Lee, Y.-M.; Luchinat, C.; Mangani, S.; Terni, B.; Turano, P. *Proc. Natl. Acad. Sci. U.S.A.* **2005**, *102*, 5334–5339.
23. Lang, R.; Kocourek, A.; Braun, M.; Tschesche, H.; Huber, R.; Bode, W.; Maskos, K. *J. Mol. Biol.* **2001**, *312*, 731–742.
24. Hajduk, P. J.; Sheppard, G.; Nettlesheim, D. G.; Olejniczak, E. T.; Shuker, S. B.; Meadows, R. P.; Steinman, D. H.; Carrera, G. M.; Marcotte, P. A.; Severin, J.; Walter, K.; Smith, H.; Gubbins, E.; Simmer, R.; Holzman, T. F.;

- Morgan, D. W.; Davidsen, S. K.; Summers, J. B.; Fesik, S. W. *J. Am. Chem. Soc.* **1997**, *119*, 5818–5827.
25. Mitton-Fry, R. M.; Anderson, E. M.; Hughes, T. R.; Lundblad, V.; Wuttke, D. S. *Science* **2002**, *296*, 145–147.
26. Knight, C. G.; Willenbrock, F.; Murphy, G. *FEBS Lett.* **1992**, *296*, 263–266.
27. Pellicchia, M.; Becattini, B.; Crowell, K. J.; Fattorusso, R.; Forino, M.; Fragai, M.; Jung, D.; Mustelin, T.; Tautz, L. *Expert Opin. Ther. Targets* **2004**, *6*, 597–611.
28. Shuker, S. B.; Hajduk, P. J.; Meadows, R. P.; Fesik, S. W. *Science* **1996**, *274*, 1531–1534.
29. Guarna, A.; Bucelli, I.; Machetti, F.; Menchi, G.; Occhiato, E. G.; Scarpi, D.; Trabocchi, A. *Tetrahedron* **2002**, *58*, 9865–9870.
30. Trabocchi, A.; Cini, N.; Menchi, G.; Guarna, A. *Tetrahedron Lett.* **2003**, *44*, 3489–3492.
31. Campestre, C.; Agamennone, M.; Tortorella, P.; Prezioso, S.; Biasone, A.; Gavazzo, E.; Pochetti, G.; Mazza, F.; Hiller, O.; Tschesche, H.; Consalvi, V.; Gallina, C. *Bioorg. Med. Chem. Lett.* **2006**, *16*, 20–24.
32. Morris, G. M.; Goodsell, D. S.; Halliday, R. S.; Huey, R.; Hart, W. E.; Belew, R. K.; Olson, A. J. *J. Comput. Chem.* **1998**, *19*, 1639–1662.
33. Gasteiger, J.; Marsili, M. *Tetrahedron* **1980**, *36*, 3219–3228.
34. Banci, L.; Bertini, I.; Ciulli, A.; Fragai, M.; Luchinat, C.; Terni, B. *J. Mol. Catal. A: Chem.* **2003**, *204–205*, 401–408.
35. Sattler, M.; Schleucher, J.; Griesinger, C. *Prog. Nucl. Magn. Reson. Spectrosc.* **1999**, *34*, 93–158.
36. Leslie, A. G. W. In *Crystallographic Computing V*; Moras, D., Podjarny, A. D., Thierry, J. C., Eds.; Molecular Data Processing; Oxford University: Oxford, 1991; pp 50–61.
37. Evans, P. R. Data Reduction, Proceedings of CCP4 Study Weekend. Data Collection & Processing, 1993, pp 114–122.
38. Rossmann, M. G.; Blow, D. M. *Acta Crystallogr.* **1962**, *D 15*, 24–31.
39. Crowther, R. A. In *The Molecular Replacement Method*; Rossmann, M. G., Ed.; Gordon & Breach: New York, 1972.
40. Vagin, A.; Teplyakov, A. *J. Appl. Crystallogr.* **1997**, *30*, 1022–1025.
41. Vagin, A.; Teplyakov, A. *Acta Crystallogr.* **2000**, *D 56*, 1622–1624.
42. Murshudov, G. N.; Vagin, A. A.; Dodson, E. J. *Acta Crystallogr.* **1997**, *D 53*, 240–255.
43. McRee, D. E. *J. Mol. Graph.* **1992**, *10*, 44–47.
44. Lamzin, V. S.; Wilson, K. S. *Acta Crystallogr.* **1993**, *D 49*, 129–147.
45. Laskowski, R. A.; MacArthur, M. W.; Moss, D. S.; Thornton, J. M. *J. Appl. Crystallogr.* **1993**, *26*, 283–291.